G3 Genes | Genomes | Genetics

INVESTIGATION

Activity-Dependent Regulation of the Proapoptotic BH3-Only Gene *egl-1* in a Living Neuron Pair in *Caenorhabditis elegans*

Jesse Cohn,* Vivek Dwivedi,† Giulio Valperga,‡ Nicole Zarate,* Mario de Bono,‡ H. Robert Horvitz,† and Jonathan T. Pierce*,1

*Department of Neuroscience; Center for Brain, Behavior and Evolution; Center for Learning and Memory; Waggoner Center for Alcohol and Addiction Research; Institute of Cell and Molecular Biology, University of Texas at Austin, Austin, Texas, †Howard Hughes Medical Institute, Department of Biology, Massachusetts Institute of Technology, Cambridge, MA 02139, and ‡Division of Cell Biology, Medical Research Council Laboratory of Molecular Biology, Cambridge, United Kingdom

ORCID ID: 0000-0002-9619-4713 (J.T.P.)

ABSTRACT The BH3-only family of proteins is key for initiating apoptosis in a variety of contexts, and may also contribute to non-apoptotic cellular processes. Historically, the nematode *Caenorhabditis elegans* has provided a powerful system for studying and identifying conserved regulators of BH3-only proteins. In *C. elegans*, the BH3-only protein *egl-1* is expressed during development to cell-autonomously trigger most developmental cell deaths. Here we provide evidence that *egl-1* is also transcribed after development in the sensory neuron pair URX without inducing apoptosis. We used genetic screening and epistasis analysis to determine that its transcription is regulated in URX by neuronal activity and/or in parallel by orthologs of Protein Kinase G and the Salt-Inducible Kinase family. Because several BH3-only family proteins are also expressed in the adult nervous system of mammals, we suggest that studying *egl-1* expression in URX may shed light on mechanisms that regulate conserved family members in higher organisms.

KEYWORDS
BH3-only
egl-1
C. elegans
URX
apoptosis

Members of the BH3-only family of proteins are essential regulators of cell death in nearly all metazoans. Each member of this family shares the "BCL-2 homology" domain BH3, which allows them to bind the anti-apoptotic members of the BCL-2 family and block their activity, thereby initiating apoptosis (Lettre and Hengartner 2006; Giam *et al.* 2008). In mammals, there are at least eight BH3-only proteins, with some estimates ranging higher (Aouacheria *et al.* 2005; Happo *et al.* 2012). These proteins are regulated in a number of ways, such as transcriptionally (Oda *et al.* 2000; Nakano and Vousden 2001; Sturm *et al.* 2006; Borensztajn *et al.* 2007), post-transcriptionally (Ventura *et al.* 2008; Sherrard *et al.* 2017), and post-translationally (Verma *et al.* 2001; Lowman *et al.* 2010). This complex regulation allows for cells to properly induce cell death during development and in response to a wide variety of contexts and circumstances. Additionally, mounting evidence suggests that some BH3-only proteins may contribute to non-apoptotic cellular processes as well, such as glucose metabolism (Danial *et al.* 2003; Danial *et al.* 2008; Giménez-Cassina *et al.* 2014), autophagy (Maiuri *et al.* 2007; Sinha *et al.* 2008; Lindqvist *et al.* 2014), and lipid transport (Esposti *et al.* 2001). Despite their important role in initiating programmed cell death and likely other cellular processes, our understanding of the factors that regulate BH3-only proteins is incomplete.

The nematode *C. elegans* has historically played an important role in understanding the mechanisms of programmed cell death and the role of BH3-only proteins (Lettre and Hengartner 2006). Genetic screens in the 1980s and 1990s using *C. elegans* uncovered a core pathway through which programmed cell death is initiated and executed (Ellis and Horvitz 1986; Yuan and Horvitz 1990; Hengartner *et al.* 1992; Yuan and Horvitz 1992; Conradt and Horvitz 1998), the main features of which are well conserved all the way through mammals (Czabotar

doi: https://doi.org/10.1534/g3.119.400654
Manuscript received February 15, 2019; accepted for publication September 9, 2019; published Early Online September 13, 2019.

Supplemental material available at FigShare: https://doi.org/10.25387/g3.9816401.
[1]Corresponding author information: University of Texas at Austin, 2506 Speedway, C7350, NMS 5.116, Austin, TX 78712, E-mail: jonps@austin.utexas.edu

et al. 2014). The primary initiator of this cell death pathway was found to be a BH3-only protein called *egl-1* (egg-laying defective-1). A gain-of-function mutation in the regulatory region of *egl-1* causes the inappropriate death of neurons in the egg-laying circuit, while subsequent loss-of-function mutations in *egl-1* prevented this cell death (Conradt and Horvitz 1998; Conradt and Horvitz 1999). *egl-1* was found to be necessary for most developmental cell deaths in the worm, and sufficient to induce apoptosis cell-autonomously when expressed ectopically *in vivo* (Conradt and Horvitz 1998; Chang *et al.* 2006; Lomonosova and Chinnadurai 2008). So far, evidence exists for *egl-1* regulation at the transcriptional and the post-transcriptional level (Nehme and Conradt 2008; Nehme *et al.* 2010; Sherrard *et al.* 2017). By focusing on individual cells that die during development, some of the transcription factors and pathways that regulate *egl-1* transcription in apoptotic cells have been found (Ellis and Horvitz 1991; Metzstein *et al.* 1996; Conradt and Horvitz 1999; Thellmann *et al.* 2003; Liu *et al.* 2006; Potts *et al.* 2009; Hirose *et al.* 2010; Winn *et al.* 2011; Hirose and Horvitz 2013; Sherrard *et al.* 2017). Notably, homologs of nearly all of these factors have also been implicated in apoptosis in higher animals, suggesting that studying *egl-1* regulation in *C. elegans* is a fruitful approach for identifying mechanisms important in cell death pathways in other systems (Wallis *et al.* 1999; Xu *et al.* 1999; Ginsberg 2002; Ruiz I Altaba *et al.* 2002; Wu *et al.* 2005; Deniaud *et al.* 2006; Wong *et al.* 2007; Sitwala *et al.* 2008).

Here we describe the first non-apoptotic example of endogenous *egl-1* transcription in living neurons in *C. elegans* after development. We find that *egl-1* mRNA is present in a very small subset of neurons in *C. elegans* and persists into adulthood – most consistently and reliably in the neuron pair URX, the main oxygen sensing neurons in *C. elegans*. The URX neurons are necessary for worms to orient properly to different oxygen levels in their environment (Gray *et al.* 2004; Zimmer *et al.* 2009; Busch *et al.* 2012), and are also involved in other various aspects of worm physiology such as fat homeostasis and immune responses (Styer *et al.* 2008; Witham *et al.* 2016). URX senses oxygen via a heterodimer of soluble guanylyl-cyclases, GCY-35 and GCY-36, which produces cGMP in response to binding oxygen. This cGMP then gates calcium currents via the cyclic-nucleotide gated ion channels CNG-1 and TAX-4 commensurate with the level of environmental oxygen (Gray *et al.* 2004; Busch *et al.* 2012; Couto *et al.* 2013). With the use of a fluorescent transcriptional reporter for *egl-1*, we find that sensory transduction in URX is necessary for *egl-1* transcription. This transcription can also be regulated in parallel by two protein kinases: EGL-4, the worm homolog of Protein Kinase G, and KIN-29, the worm Salt-Inducible Kinase family homolog, as well as by at least one more unknown pathway.

Because the study of *egl-1* regulation has historically yielded insight into factors that control apoptosis in higher animals, we propose that this novel adult transcription of *egl-1* in URX may further our understanding of roles and regulatory mechanisms of BH3-only proteins in apoptotic and potentially non-apoptotic contexts.

MATERIALS AND METHODS

Strains Used

The following strains were used: N2 Bristol as wild type; JPS600 *vxEx600[Pegl-1::mCherry Punc-122::GFP]*; JPS601 *vxIs601[Pegl-1::mCherry Punc-122::GFP]*; JPS602 *vxEx602[Pegl-1::mCherry Punc-122::GFP Pgcy-32::GFP]*; JPS620 *ced-6*(*n1813*) III; *vxEx602[Pegl-1::mCherry Punc-122::GFP Pgcy-32::GFP]*; MT22516 *him-8*(*e1489*) V; *nIs343[Pegl-1::4xNLS::GFP]*; MT8735 *egl-1*(*n1084n3082*) V; RB1305 *egl-1*(*ok1418*) V; AX7629 *dbEx614[Pgcy-37::YC2.60::unc-54UTR Punc-122::RFP]*; JPS1191 *egl-1*(*n1084n3082*) V; *dbEx614[Pgcy-37::YC2.60::unc-54UTR Punc-122::RFP]*; JPS879 *vxEx879[Pgcy-32::GFP Punc-122::GFP]*; JPS1106 *egl-1*(*n1084n3082*) V; *vxEx1106[Pgcy-32::GFP Pfat-7::GFP]*; JPS1031 *vxEx1031[Pgcy-32::RAB-3::GFP Pgcy-32::mCherry]*; JPS1070 *egl-1*(*n1084n3082*) V; *vxEx1031[Pgcy-32::RAB-3::GFP Pgcy-32::mCherry]*; JPS696 *cng-1*(*vx3*) V; *vxIs601[Pegl-1::mCherry Punc-122::GFP]*; JPS803 *cng-1*(*vx3*) V; *vxIs601[Pegl-1::mCherry Punc-122::GFP]*; *vxEx803[Pgcy-32::CNG-1(+) Peft-2::GFP]*; JPS793 *gcy-35*(*ok769*) I; *vxEx600[Pegl-1::mCherry Punc-122::GFP]*; JPS909 *gcy-36*(*db42*) X; *vxEx600[Pegl-1::mCherry Punc-122::GFP]*; JPS812 *egl-19*(*n582*) IV; *vxEx600[Pegl-1::mCherry Punc-122::GFP]*; JPS839 *egl-19*(*n2368*) IV; *vxEx600[Pegl-1::mCherry Punc-122::GFP]*; JPS937 *egl-4*(*n477*) IV; *vxIs601[Pegl-1::mCherry Punc-122::GFP]*; JPS1124 *kin-29*(*oy38*) X; *vxIs601[Pegl-1::mCherry Punc-122::GFP]*; JPS1040 *egl-4*(*n477*) IV; *kin-29*(*oy38*) X; *vxIs601[Pegl-1::mCherry Punc-122::GFP]*; JPS1020 *egl-4*(*n477*) IV; *muIs102[Pgcy-32::GFP]* V; JPS912 *mef-2*(*gv1*) I; *vxIs601[Pegl-1::mCherry Punc-122::GFP]*; JPS893 *egl-4*(*vx19*) IV; *cng-1*(*vx3*) V; *vxIs601[Pegl-1::mCherry Punc-122::GFP]*; JPS1190 *egl-4*(*n477*) IV; *cng-1*(*jh111*) V; *vxIs601[Pegl-1::mCherry Punc-122::GFP]*; JPS1127 *cng-1*(*jh111*) V; *kin-29*(*oy38*) X; *vxIs601[Pegl-1::mCherry Punc-122::GFP]*; JPS1126 *gcy-35*(*ok769*) I; *egl-4*(*n477*); *kin-29*(*oy38*) X; *vxIs601[Pegl-1::mCherry Punc-122::GFP]*

Molecular Biology and Transgenic Strain Construction

The *egl-1* reporter construct was generated by long PCR fusion of three fragments: 1042-bp upstream of the *egl-1* start codon amplified from N2 DNA lysate, worm-optimized mCherry amplified from plasmid pCFJ90, and 5744-bp of the 3′ downstream region of *egl-1* genomic DNA including the 3′UTR of *egl-1* amplified from N2 lysate (Shevchuk *et al.* 2004). Primers used to generate the final fused product were: AGGCCTGATCATAGTTTCTGCCATTT and ATCCCTAACATATTTCTCAAAGATACAAATGTCATC.

To generate the strain JPS601 with the integrated *egl-1* reporter transgene *vxIs601*, we first transformed the above PCR product into N2 WT by microinjection at a concentration of 2 ng/µl along with a *Punc-122::GFP* co-injection marker to generate strain JPS600 carrying the extra-chromosomal array *vxEx600*. This array was then integrated by UV irradiation using a UV Stratalinker 2400 (Stratagene), and the resulting integrated strain was then outcrossed to N2 six times before any further use (Mariol *et al.* 2013).

URX neuron labeling constructs were generated by using an 876-bp fragment of the *gcy-32* promoter established from earlier studies (Yu *et al.* 1997). The promoter fragment was amplified from N2 gDNA and then PCR fused with either worm-optimized mCherry amplified from pCFJ90 or worm-optimized GFP amplified from pPD95.75. The fused products were then subcloned into the pCR-Blunt vector using a Zero Blunt PCR Cloning Kit from ThermoFisher Scientific. These constructs were used in injection mixes at a concentration of 20 ng/µl.

The URX-targeted synaptic marker RAB-3::GFP was generated by digesting plasmid NM1028 with *Pst*I and *Nco*I and inserting the *gcy-32* promoter with Gibson Assembly. This construct was injected at a concentration of 25 ng/µl. NM1028 was a kind gift of Michael Nonet (Washington University in St. Louis).

The construct to cell-specifically rescue *cng-1* in URX was generated by amplifying the full coding region of *cng-1* and the *gcy-32* promoter each from N2 gDNA. These were then assembled by Gibson Assembly with a pPD95.75 backbone that had been digested with *Xba*I and *Eco*RI. This was then injected at a concentration of 20 ng/µl.

Mutations were followed in crosses by PCR genotyping and/or by phenotype where applicable.

Mutagenesis and Mutant Identification

To screen for mutations that affect expression of *vxIs601* in URX, we mutagenized the otherwise wild-type strain JPS601 with 0.5-mM N-ethyl-N-nitrosourea (ENU) in M9 buffer for 4 hr and then examined F2 progeny using a fluorescence dissection microscope. We looked for animals with a loss or diminishment of mCherry expression in URX. We followed the strategy outlined in Zuryn, *et al.* (2010), to identify candidate causal mutations. We identified allele *vx3* as an A-to-C mutation 651 bp from the start codon of *cng-1* predicted to convert the aspartic acid at position 162 to an alanine.

For our reversion screen, *cng-1(vx3)* mutant animals were backcrossed to strain JPS601 six times and then subjected to ENU treatment as above. F2 progeny were screened on a fluorescence dissection microscope to look for recovery of fluorescence in URX. All revertant mutants displayed a slight egg-laying defect and a longer body than wild type – common characteristics of the *egl-4* mutant. Revertant mutants failed to complement the *egl-4(n477)* allele when tested for *vxIs601* expression in URX. One member of this complementation group, *vx19*, showed a T-to-G early stop-codon mutation at position 2389 of the *egl-4 F55A8.2a.1* transcript. This mutation truncates the final 18 amino acids from the protein.

General Microscopy

Worms were mounted on 2% agarose pads and anesthetized with 30-mM sodium azide in NGM. Epifluorescent images were taken on an Olympus IX51 inverted microscope equipped with an X-Cite FIRE LED Illuminator (Excelitas Technologies Corp.) using an Olympus UPlanFL N 40X/0.75 NA objective and QCapture Pro 6.0 software. Confocal images were taken with a Zeiss LSM 710 microscope equipped with a Plan-Apochromat 40x/1.4 Oil objective and Zen Software.

egl-1 Reporter Fluorescence Quantification and Oxygen Experiments

For fluorescence quantification of the *egl-1* reporter in URX, animals were synchronized by timed egg laying and then imaged three days later. *kin-29* mutants develop significantly slower than wild-type worms or *egl-4* mutants, however because reporter expression level is a function of the amount of time an animal is exposed to oxygen as opposed to a particular age, we compared day 1 wild-type and *egl-4* adults to L2-L3 *kin-29* animals that had been synchronized by egg-laying.

Fluorescence intensity was quantified with FIJI software as previously described (Mccloy *et al.* 2014). Briefly, the cell body was outlined and then the background was subtracted to give a final fluorescence intensity for each cell. These values were then normalized to wild-type animals grown in parallel at 21% oxygen for comparison purposes. Pictures shown in figures are to show presence/absence of reporter expression; non-saturated photos were used for quantification.

For experiments in which the oxygen environment was different than 21%, worms were grown or maintained in a Modular Incubator Chamber (Billups-Rothenberg) attached to oxygen tanks containing 100% medical grade O_2 (Praxair), or either 1% or 10% O_2 balanced with nitrogen (Airgas).

Single Molecule FISH

smFISH experiments were performed as described elsewhere (Raj *et al.* 2008). Fixed mixed stage animals were incubated overnight at 30° with previously designed *egl-1* probes (Johnsen and Horvitz 2016). Animals were subsequently mounted for imaging after two washes lasting 30 min each. Image acquisition was performed on a Nikon TE-2000 inverted microscope with a 100x objective (Nikon, NA 1.4). A Pixis 1024 camera (Princeton Instruments) controlled by MetaMorph software (Molecular Devices) was used to detect smFISH signal and acquire images with an exposure time of 2 sec. Images were processed and prepared for publication using ImageJ software (NIH).

URX Calcium Imaging

To image young adults, we picked L4 animals expressing the YC2.60 Ca^{2+} sensor 24 hr before imaging. On the day of the assay, 5 – 10 day 1 adult animals were glued to agarose pads (2% in M9 buffer, 1 mM $CaCl_2$), using Dermabond tissue adhesive, with their body immersed in OP50 washed off from a seeded plate using M9 buffer. The animals were quickly covered with a PDMS microfluidic chamber and 7% O_2 was pumped into the chamber for 2 min before we began imaging, to allow animals to adjust to the new conditions. Neural activity was recorded for 9 min with switches in O_2 concentration every 2 min.

Imaging was performed on an AZ100 microscope (Nikon) bearing a TwinCam adaptor (Cairn Research, UK), two ORCAFlash4.0 V2 digital cameras (Hamamatsu, Japan), and an AZ Plan Fluor 2× lens with 2× zoom. Recordings were at 2Hz. Excitation light from a Lambda LS xenon arc lamp (Sutter) was passed through a 438/24 nm filter and an FF458DiO2 dichroic (Semrock). Emitted light was passed to a DC/T510LPXRXTUf2 dichroic filter in the TwinCam adaptor cube and then filtered using a 483/32 nm filter (CFP), or 542/27 nm filter (YFP) before collection on the cameras. Recordings were analyzed using Neuron Analyzer, a customwritten Matlab program available at https://github.com/neuronanalyser/neuronanalyser.

Lifespan Assays on Pseudomonas aeruginosa

Assays were performed as previously described (Styer *et al.* 2008). *P. aeruginosa* was grown overnight at 37° and then seeded onto NGM-agar plates modified to contain 0.35% peptone. After seeding, plates were placed at 37° overnight and moved in the morning to 25° to equilibrate temperature. At least 10 gravid adults were placed on each plate with 4-5 replicate plates per strain per assay. Animals were assessed every 4-8 hr for survival. Those that failed to respond to touch were counted as dead, and animals that crawled up the sides of the plate and desiccated were censored. Animals were maintained at 25° and moved to fresh plates every other day over the course of the assay.

Dendrite Scoring Assays

URX dendrites in day 4 adults carrying a *Pgcy-32::GFP* transgene were visualized and scored for tip morphology. Dendritic endings with a secondary branch that extended at least 5 microns from the primary branch were scored as "complex", otherwise they were scored as "simple". About 17% of URX dendrites in the *egl-1* mutant failed to extend all the way to the tip of the nose, possibly because of extra undead cells interfering with dendritic attachments to glia. These animals were not included in the determination of complex/simple ratios.

Data Availability

Strains and plasmids are available upon request. The authors affirm that all data necessary for confirming the conclusions of the article are present within the article and figures. Supplemental material available at FigShare: https://doi.org/10.25387/g3.9816401.

RESULTS

egl-1 is transcribed in URX neurons post-developmentally

To investigate the expression pattern of *egl-1*, we generated a transcriptional reporter construct consisting of 1.1 kb of the upstream promoter region, as well as 5.5 kb of the region downstream of the gene.

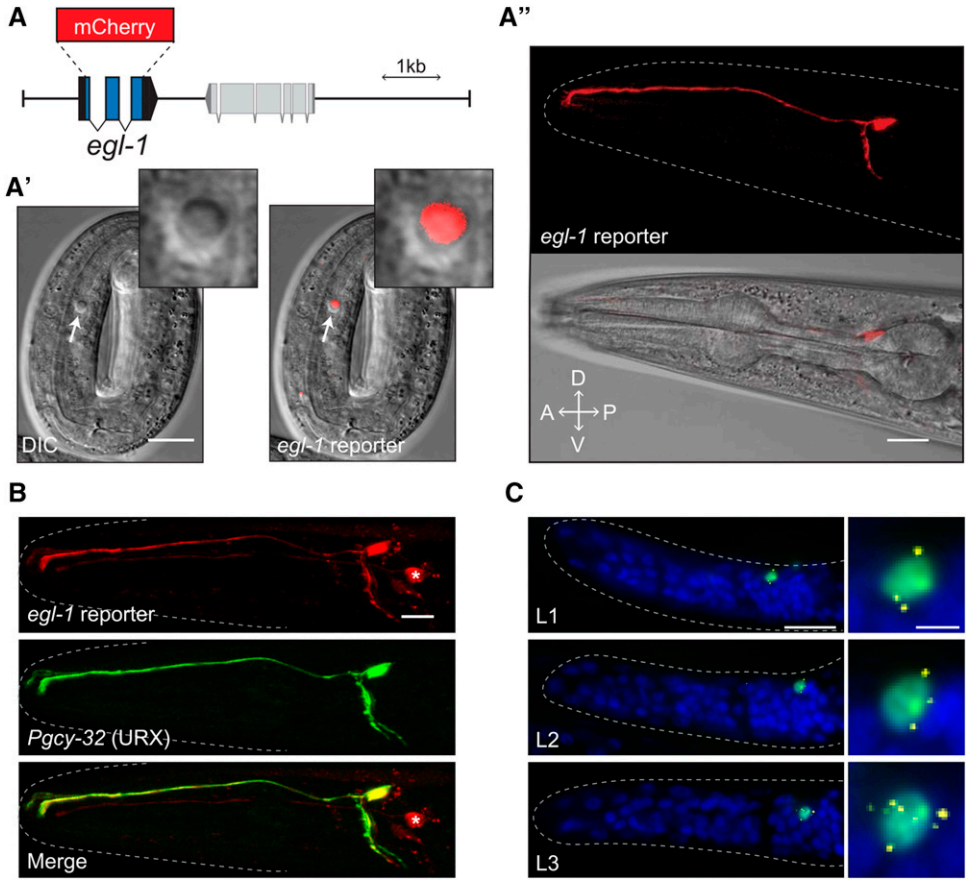

Figure 1 The BH3-only gene *egl-1* is transcribed post-developmentally in the URX neuron pair. A. Schematic representation of the *egl-1* reporter construct in which the *egl-1* coding sequence is replaced with *mCherry*. A'. Expression of the *egl-1* reporter construct in a *ced-6(n1813)* embryo in which dead cell corpses persist. Arrows and inset show an apoptotic cell corpse that expresses the *egl-1* reporter. A''. Example of *egl-1* reporter expression in a day 2 adult wild-type worm. B. Overlapping expression of the *egl-1* reporter and a *Pgcy-32::GFP* reporter that labels the URX neuron pair. Asterisk indicates expression of the *egl-1* reporter in cells other than URX that occasionally occurs. C. Single molecule fluorescent *in situ* hybridization (smFISH) showing *egl-1* transcripts in animals carrying the *nIs343* transgene (*Pegl-1::4xNLS::GFP*). Blue is DAPI, *egl-1* mRNA transcripts are labeled yellow, green is GFP. Larval age of each animal is shown in white text. All scale bars are 10 μm, except for the enlargements in C in which the scale bar is 2 μm.

The coding region of *egl-1* was replaced with a *C. elegans*-optimized version of mCherry (Figure 1A). We integrated this construct to create the transgenic reporter *vxIs601* (Mariol *et al.* 2013). To ensure that *vxIs601* faithfully reported true *egl-1* expression, we visualized apoptotic cells in a *ced-6(n1813)* mutant background in which dead cell corpses persist due to a defect in engulfment (Figure 1A') (Liu and Hengartner 1998). We found that apoptotic cell corpses reliably showed high mCherry expression, indicating that *vxIs601* correctly reflects *egl-1* transcription in at least the developmental cell deaths we examined. For simplicity and clarity, we refer to *vxIs601* as the *egl-1* reporter from hereon.

To our surprise, we also found that the *egl-1* reporter was expressed in adult animals in a very small subset of neurons, and in one pair especially strongly in all individuals (Figure 1A''). This expression persisted throughout the entire life of the worm. We used cell-specific reporters and morphological characterization to identify the neurons most brightly expressing the reporter as the bilaterally symmetric neuron pair URX (Figure 1B) (Yu *et al.* 1997). By examining eggs, we found that *egl-1* reporter expression was detectable in URX by at least the threefold stage, albeit at extremely faint levels compared to later expression (Supplemental Figure 1). In addition to URX, we also found that AQR, PQR and one of the AWCon/off neuron pair expressed the reporter less often (see Figure 1B, top, for an example). Of these neurons, the expression in the URX neuron pair was the most consistent and robust, so we chose to characterize the adult expression of *egl-1* by focusing our attention specifically on URX.

Reporter genes are occasionally expressed in cells that do not normally express the endogenous gene because the reporter lacks regulatory regions that repress the endogenous gene (Tursun *et al.* 2009). To test this possibility for our *egl-1* reporter, we used single molecule fluorescence *in-situ* hybridization (smFISH) to confirm whether endogenous *egl-1* mRNA transcripts could be found in URX (Johnsen and Horvitz 2016). To test the co-localization of the *egl-1* fluorescent reporter and endogenous *egl-1* mRNA, we used animals that carry the *egl-1* reporter transgene *nIs343*, which expresses nuclear-localized GFP using 6.5 kb of the upstream promoter region of *egl-1* (Hirose and Horvitz 2013). These animals showed the same expression pattern as our *egl-1* reporter described above (*vxIs601*), including expression of GFP in a small number of neurons persisting past development, and especially strongly in URX. We found that the GFP expression always (8/8 worms) co-localized with the smFISH signal from probes targeted to the *egl-1* transcript (Figure 1C). Notably, this expression continued past the L2 larval stage, which is when the last somatic cell deaths in the hermaphrodite occur (Sulston and Horvitz 1977).

Past studies have identified genomic regulatory regions around *egl-1* that control expression in certain apoptotic cells, so we performed promoter truncation experiments to determine whether *egl-1* expression in URX is dependent on regions previously identified as important for *egl-1* transcription in other cells (Boulin *et al.* 2006). We identified a 20-bp region ~85 bp upstream from the *egl-1* transcriptional start site that was necessary for reporter expression in URX (Figure S1). This region has not been identified as necessary for any cell deaths examined in the worm thus far, and it is near but distinct from a previously identified binding site of the transcription factor SPTF-3 (Hirose and Horvitz 2013). This suggests that *egl-1* transcription is regulated in URX by different regulatory regions than have been previously described in developmental cell deaths, though this area may still be necessary for *egl-1* expression during development in cells other than URX.

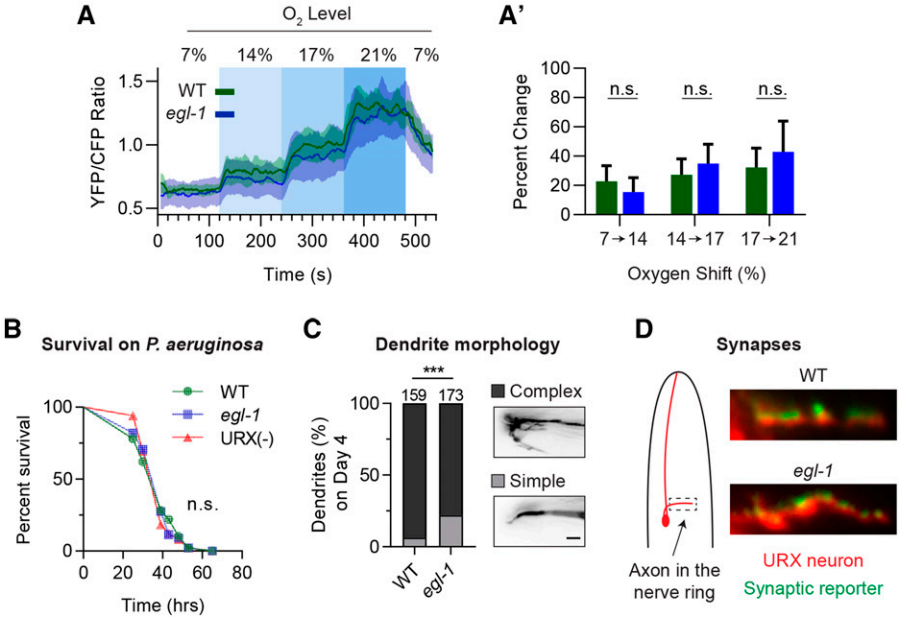

Figure 2 Analysis of URX- and *egl-1*-related phenotypes in wild-type and *egl-1* mutant worms. A. Calcium imaging of URX oxygen responses in day 1 adult wild type (n = 23) and *egl-1(n1084n3082)* (n = 22) worms. Each strain expresses the ratiometric calcium sensor YC2.60 in URX, and images of the cell body were captured at a rate of 2 Hz. Increased YFP/CFP ratio reflects increased intracellular calcium. Shaded regions indicate 95% confidence intervals. A'. Percent changes in intracellular calcium in URX from each step change in panel A. The YFP/CFP ratio at each oxygen level was calculated by averaging the final 30 sec prior to stimulus change. The percent changes in intracellular calcium in wild type and *egl-1(n1084n3082)* worms showed no significant differences as determined by Bonferroni corrected multiple *t*-tests. Error bars are 95% confidence intervals. B. Lifespan of worms transferred as day 1 adults to pathogenic *Pseudomonas aeruginosa*. URX(-) worms carry the *qaIs2241* transgene which genetically ablates URX, AQR, and PQR by overexpressing *egl-1* in those cells. Wild type (n = 50) *vs.* *egl-1(ok1418)* (n = 45) *vs.* URX(-) (n = 49), $P = 0.99$ as determined by the Mantel-Cox test. C. Dendritic morphology assay of day 4 adults. Complex dendrites have at least one secondary branch that extends at least 5 μm from the primary dendritic stalk, simple dendrites do not. Wild-type (n = 159) *vs.* *egl-1(n1084n3082)* (n = 173), $P < 0.01$ as determined by Fisher's exact test. D. Representative photos of URX synapses (green) in wild type and *egl-1(n1084n3082)* day 1 adults. Both strains carry a *[Pgcy-32::mCherry Pgcy-32::RAB-3::GFP]* reporter transgene. Arrows point to the URX axon (red) in the nerve ring. All scale bars are 5 μm.

We tried several approaches to determine whether the EGL-1 protein was also produced in URX; however, due to technical difficulties we were unable to make this assessment (see Discussion for more details). Nevertheless, we conclude that endogenous *egl-1* is transcribed post-developmentally in the URX neuron pair without initiating apoptosis.

No obvious role for *egl-1* in URX neurons

The URX neurons do not die under normal conditions. This leaves open the possibility that *egl-1* may play a non-apoptotic role in URX. To address this hypothesis, we examined the *egl-1* loss-of-function mutant with regard to a variety of URX- and *egl-1*-related phenotypes. We examined either the loss-of-function *egl-1(n1084n3082)* allele, which has an insertion that causes a frameshift and loss of the BH3 domain of the protein, or the presumed null *egl-1(ok1418)* allele which deletes a portion of the *egl-1* promoter and coding region.

URX is the main class of oxygen-sensing neurons in *C. elegans*. Increases in environmental oxygen lead to increases in calcium influx into the neurons, which can be measured by expressing the ratiometric calcium sensor YC2.60 in URX (Nagai *et al.* 2004). We tested whether *egl-1* plays a role in oxygen sensation in URX by comparing oxygen responses in wild-type and *egl-1(n1084n3082)* mutant day 1 adults (Figure 2A and 2A'). We exposed worms to several oxygen concentrations ranging from 7 to 21% oxygen, but found no significant difference in the URX oxygen response of *egl-1* mutant worms at any oxygen level we tested. We conclude from these results that *egl-1* is not involved in oxygen sensation in URX.

URX has also been suggested to have a role in the *C. elegans* innate immune response. Transgenic worms lacking the URX, AQR, and PQR neurons were shown to survive longer than wild-type animals on the pathological bacteria *Pseudomonas aeruginosa* (Styer *et al.* 2008). We found that the *egl-1(ok1418)* mutant has similar survival rates as wild type on *P. aeruginosa* (Figure 2B), though we note that we were unable to replicate the previous finding that worms lacking URX, AQR, and PQR survive longer on *P. aeruginosa*, despite several attempts. Thus, we cannot definitively conclude whether *egl-1* is necessary for URX to contribute to the innate immune response in *C. elegans*; however, we think it is unlikely that *egl-1* plays this role. We also examined URX morphology to look for any signs of neurodegeneration after incubation for 24 hr on *P. aeruginosa*, but found no obvious defects in any worms (40/40).

URX has been described as having a characteristic variable, branched dendritic ending at the tip of the nose ("complex" endings) (Ward *et al.* 1975; White *et al.* 1986; Doroquez *et al.* 2014). In our parallel submitted work, we show that URX dendritic tips fail to branch in certain genetic and environmental conditions ("simple" endings). We examined the *egl-1(n1084n3082)* mutant for dendritic tip morphology and found that it had "simple", unbranched tips more often than wild-type animals (22% simple *vs.* 6.3% simple, $P < 0.01$ Fisher's exact test) (Figure 2C). However, the effect size was much smaller relative to what we found in other genetic background and environmental conditions. Moreover, the effect could be due to a number of other factors such as supernumerary cells in the head region of the *egl-1* mutant interfering with proper tip elaboration in certain individuals, so we did not characterize this phenotype further in the *egl-1* mutant.

Finally, *egl-1* has previously been suggested to have a role in synapse pruning during the development of the RME neurons (Meng *et al.* 2015). Using a GFP-tagged version of the synaptic marker RAB-3 expressed specifically in the URX neurons (Bounoutas *et al.* 2009), we visually compared URX synapses in the nerve ring in wild type and the *egl-1(n1084n3082)* mutant, but found no gross defects in synapse localization or abundance in the *egl-1* mutant (Figure 2D). This suggests that *egl-1* does not play an obvious role in synapse pruning in URX under basal circumstances.

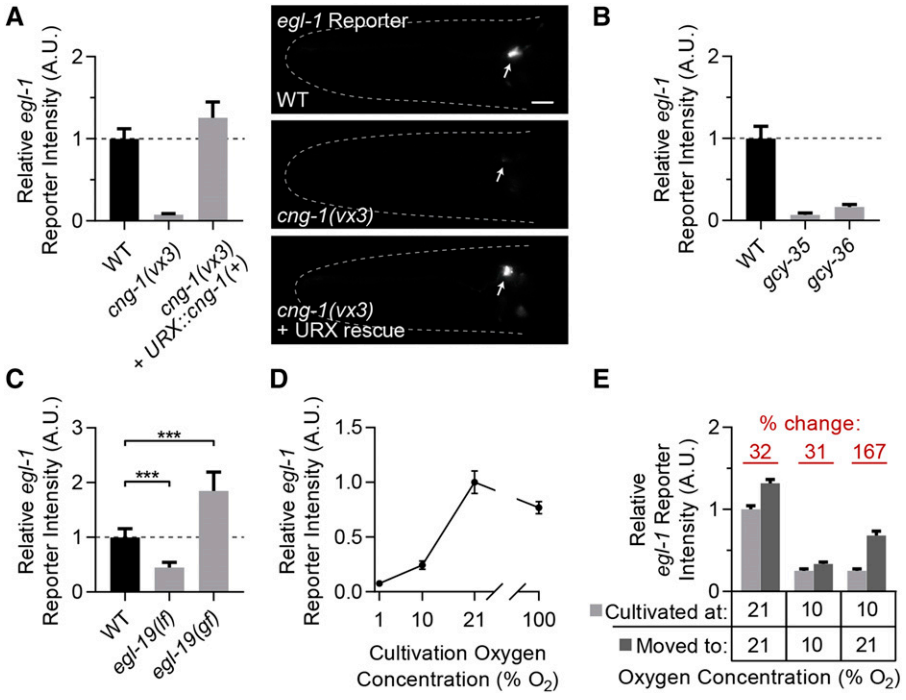

Figure 3 Neuronal activity drives expression of the *egl-1* reporter in the oxygen-sensing URX neurons. A. *egl-1* reporter expression in day 1 wild-type, *cng-1(vx3)*, and *cng-1(vx3)* worms carrying a *Pgcy-32::cng-1(+)* rescuing transgene that expresses only in URX, AQR and PQR. All animals were grown at 21% oxygen. Values are normalized to wild type. n ≥ 30 worms per genotype. Representative images are shown to the right; arrows indicate the URX cell body, scale bar is 10 μm. B. *egl-1* reporter expression in day 1 wild-type worms and *gcy-35(ok769)* or *gcy-36(db42)* mutants lacking components of the oxygen-sensing GCY-35/GCY-36 complex grown at 21% oxygen. Values are normalized to wild type. n ≥ 30 worms per genotype. C. *egl-1* reporter expression in day 1 wild type, *egl-19(n582lf)*, and *egl-19(ad2368gf)* worms. Values are normalized to wild type. $P \geq 0.01$ compared to wild type for both as determined by Student's *t*-test, n ≥ 50 worms per genotype. D. *egl-1* reporter expression in wild-type worms grown until day 1 of adulthood in the indicated oxygen level. Values are normalized to wild-type grown at 21% oxygen. n ≥ 60 worms per condition. E. Wild-type populations were reared at the "cultivated at" oxygen level until day 1 of adulthood when *egl-1* reporter expression was quantified. Plates were then moved to the "moved to" oxygen conditions until day 2 of adulthood and *egl-1* reporter expression was again quantified. Bars represent pooled results from three separate trials run on different days, n ≥ 170 worms per condition. All error bars are 95% C.I.

egl-1 expression in URX neurons is activity dependent

Given that previous studies of *egl-1* transcriptional regulation have revealed conserved regulators that are involved in apoptosis in higher organisms, and the novel non-apoptotic nature of the *egl-1* transcription in URX, we set out to characterize how this transcription was controlled. We used the *egl-1* reporter to conduct an unbiased forward genetic screen looking for mutants in which mCherry fluorescence was diminished or lost in URX. We recovered several mutants, including a missense mutation in *cng-1* (Cho *et al.* 2005; Wojtyniak *et al.* 2013). The *vx3* allele of *cng-1* is an A-to-C transversion in the third exon, changing an aspartic acid to an alanine. We confirmed the causal nature of this mutation by cell-specific rescue in URX (Figure 3A), and by phenocopy with the canonical *jh111* deletion allele of *cng-1* (data not shown).

CNG-1 is a cyclic nucleotide-gated ion channel that is an essential component of the oxygen sensation pathway in URX (Busch *et al.* 2012; Couto *et al.* 2013). Thus, we hypothesized that perhaps *egl-1* expression was driven by oxygen sensation and neuronal activity. We tested this hypothesis by quantifying reporter expression in other mutants defective in oxygen sensation, as well as in wild-type worms maintained in varying levels of environmental oxygen.

First, we quantified *egl-1* reporter expression in mutants lacking *gcy-35* or *gcy-36*. These genes encode soluble guanylyl-cyclases that heterodimerize and produce cGMP in response to binding molecular oxygen (Cheung *et al.* 2004). Both *gcy-35* and *gcy-36* are necessary for URX to respond to changes in environmental oxygen. We found that both *gcy-35(ok769)* and *gcy-36(db42)* loss-of-function mutants had a near complete lack of *egl-1* reporter expression in URX (Figure 3B).

Prolonged calcium entry into URX through CNG-1 in response to long-term oxygen sensation eventually gates the only L-type voltage-gated calcium channel in *C. elegans*, EGL-19 (Busch *et al.* 2012). We tested a role for EGL-19 in *egl-1* expression in URX by quantifying *egl-1* reporter expression in both a loss-of-function allele of *egl-19*, as well as a gain-of-function allele which has an increased open probability (Lainé *et al.* 2014). We found that *egl-1* reporter expression in URX was significantly decreased in the *egl-19(n582)* loss-of-function allele, and significantly increased in the *egl-19(n2368)* gain-of-function allele. These results signify that EGL-19 activation downstream of prolonged oxygen sensation is necessary for *egl-1* transcription in URX (Figure 3C).

We next directly assessed whether environmental oxygen sensation drives *egl-1* expression in URX by cultivating wild-type animals with the *egl-1* reporter in different oxygen environments and quantifying reporter expression on day 1 of adulthood. Wild isolates of *C. elegans* have a preference for 5–12% O_2 conditions, which is thought to reflect the environments most favorable to their survival (Gray *et al.* 2004). These strains will avoid both hypoxia (<1% O_2) and oxygen levels over 12% O_2, including the 21% O_2 conditions normally found at the lab benchtop. The lab strain N2 has a dampened capability to avoid 21% oxygen due to a gain-of-function mutation in the gene *npr-1* (De Bono and Bargmann 1998). This difference in behavior is not explained by differences in the URX neuron itself however, as both N2 and the *npr-1* loss-of-function mutant (which mimics the *npr-1* allele found in natural isolates) display similar URX calcium dynamics in response to oxygen (Jang *et al.* 2017). Instead, the difference in behavior is thought to originate from functional differences downstream of URX. For these reasons, we grew N2 animals in 1%, 10%, or 21% oxygen environments. We also grew worms in 100% oxygen to test whether the *egl-1* reporter would be expressed higher than at 21% conditions, and may possibly lead to cell death of URX. This oxygen condition is likely much higher than worms experience in their natural environment.

We found that *egl-1* reporter expression levels reflected the cultivation level of oxygen up to 21% oxygen, with day 1 animals grown in 1% oxygen having only eight percent the level of reporter expression as those grown in 21% oxygen (Figure 3D). Interestingly, worms grown at 100% oxygen actually had slightly lower expression of the reporter than those grown at 21%, and the morphology of URX was normal in these worms.

We considered the possibility that growth from egg to adulthood in these different environments had caused developmental differences in the URX neuron that led to the differences we observed in reporter expression. Therefore, we carried out a complementary set of experiments where populations were grown at one oxygen concentration until day 1 of adulthood and then shifted to another oxygen level until day 2. Worms grown at 10% or 21% oxygen, and then maintained at those same levels until day 2 had an increase of reporter expression of about thirty percent over that period, while populations grown at 10% oxygen then moved to 21% oxygen had a mean increase of over 150% from day 1 to day 2 (Figure 3E). Taken together, these experiments strongly suggest that environmental oxygen sensation by URX is necessary for expression of *egl-1* in URX.

EGL-4 and KIN-29 regulate *egl-1* expression in URX partially in parallel

We undertook two approaches to identify other genetic pathways that may regulate *egl-1* expression in URX: a reversion screen where we screened for mutants that recovered *egl-1* reporter expression in a *cng-1(vx3)* mutant background, and a candidate screen focused on other genes known to regulate activity-dependent genes.

Our reversion screen recovered several alleles of *egl-4*, the worm homolog of Protein Kinase G, as determined by complementation tests and phenocopy (Daniels *et al.* 2000; Stansberry *et al.* 2001; L'etoile *et al.* 2002). We sequenced the *egl-4* genomic area in one of these recovered mutants, *vx19*, and found a T-to-G transversion that introduces a stop codon eliminating the final 18 amino acids of the protein. This region is part of the "AGC-kinase C-terminus" domain, which is shared among related kinases and is highly conserved through humans (Parker and Parkinson 2001). Both *egl-4(n477);cng-1(jh111)* double and *egl-4(n477)* loss-of-function single mutants expressed the *egl-1* reporter higher than wild type, though expression was decreased in the double mutant compared to the *egl-4* single mutant (Figure 4A, 4D). This indicates that EGL-4 likely acts partially in parallel with CNG-1 and functions to repress expression of *egl-1*. This is consistent with past studies that have outlined how EGL-4 translocates into the nucleus to affect gene expression in response to long-term neuronal activity (O'Halloran *et al.* 2012). We confirmed expression of *egl-1* in URX in the *egl-4(n477)* mutant by smFISH (Figure 4B), further affirming the fidelity of the *egl-1* reporter to endogenous *egl-1* transcription.

Separately, we also examined *egl-1* reporter expression in another kinase pathway mutant that has been previously implicated in regulating activity-dependent gene expression. KIN-29 is the worm homolog of the Salt-Inducible Kinase (SIK) family of proteins, and like EGL-4, has been shown to translocate to the nucleus to affect gene transcription in certain contexts (Katoh *et al.* 2002; Van Der Linden *et al.* 2007; Van Der Linden *et al.* 2008). We found that the *kin-29(oy38)* loss-of-function mutant had increased *egl-1* reporter expression in URX compared to wild-type, though less than the *egl-4* mutant (Figure 4A).

EGL-4 and KIN-29 have previously been shown to regulate expression of the *str-1* chemoreceptor in the AWB sensory neuron by phosphorylating the MEF-2 transcription factor, antagonizing its activity (Van Der Linden *et al.* 2007). If MEF-2 were also involved in expression of *egl-1* in URX, we would expect it to have the opposite phenotype of EGL-4, which would be decreased expression of the *egl-1* reporter at 21% oxygen. However, the *mef-2(gv1)* loss-of-function mutant had the same level of *egl-1* reporter expression as wild type (Figure 4C). This suggests that EGL-4 likely does not act through MEF-2 in regulating *egl-1* expression as it does *str-1*.

Several pieces of evidence suggest that *egl-4* and *kin-29* act at least partially in parallel to regulate *egl-1* transcription in URX. First, we found that the *egl-4;kin-29* double mutant had higher *egl-1* reporter expression than either single mutant (Figure 4A). Reporter intensity at 21% oxygen normalized to wild type was 10.7 ± 2.6 (st. dev.) for the *egl-4;kin-29* double mutant, compared to 5.0 ± 1.0 for *egl-4* and 2.7 ± 0.6 for *kin-29* single mutants. Also, we found that the *cng-1;kin-29* double mutant had very low expression of the *egl-1* reporter, in contrast to the *egl-4;cng-1* double mutant which had higher expression of the reporter than wild type (Figure 4D). These results strongly suggest that *egl-4* and *kin-29* act through partially separate pathways to repress expression of *egl-1* in URX.

Above, we found that the *egl-1* reporter was expressed higher than wild type in the *egl-4* mutant even when the URX oxygen transduction pathway was severely compromised with the *cng-1* mutation. This made us wonder whether environmental oxygen could still regulate *egl-1* transcription in URX in mutants without the *egl-4* and *kin-29* repressor pathways. We hypothesized that the *egl-1* reporter would be expressed highly even at low oxygen in these mutants. However we found that *egl-4* and *kin-29* single mutants as well as the *egl-4;kin-29* double mutant still showed decreased reporter expression in low oxygen conditions (Figure 4E). This provides evidence for at least a third, oxygen-dependent mechanism to regulate *egl-1* expression in URX. As an independent test for this hypothesis, we asked if the *egl-1* reporter was still expressed in *egl-4;kin-29* after mutation of the oxygen sensor GCY-35. We found that the triple mutant *gcy-35;egl-4;kin-29* showed vastly decreased reporter expression compared to the *egl-4;kin-29* double mutant (Figure 4F). Interestingly, the triple mutant still had reporter expression at about wild-type levels, and higher than the *gcy-35* single mutant. These results are most consistent with the possibility that GCY-35 is upstream of at least one repressive pathway other than the *egl-4* and *kin-29* pathways, and that this unknown pathway can regulate *egl-1* expression in URX in an oxygen-dependent manner (Figure 4G).

DISCUSSION

egl-1 is transcribed in the URX neurons post-developmentally without killing them

Here we described the unexpected transcription of the proapoptotic BH3-only gene *egl-1* in the URX neuron pair in post-developmental *C. elegans*. We also note that while this paper was under review, Taylor, *et al.* published the first single-cell resolution transcriptome of L4-larval stage *C. elegans* (Taylor *et al.* 2019). Out of all of the cells analyzed, this data set reports the highest expression of *egl-1* in URX, and to a lesser extent in AWC/off, AQR, PQR and AIA neurons. This independent approach strikingly confirms the expression pattern that we found for *egl-1* using transcriptional reporters and smFISH.

This expression of *egl-1* in URX is unusual because it stands in contrast to the typical context of *egl-1* expression, which mostly occurs during development to trigger apoptosis. Previous work has suggested that both pro- and anti-apoptotic genes are present in developing cells (Shaham and Horvitz 1996). They function antagonistically, keeping a cell alive unless the apoptotic cascade is initiated by *egl-1* expression. However, *egl-1* transcription in URX, which continues past when

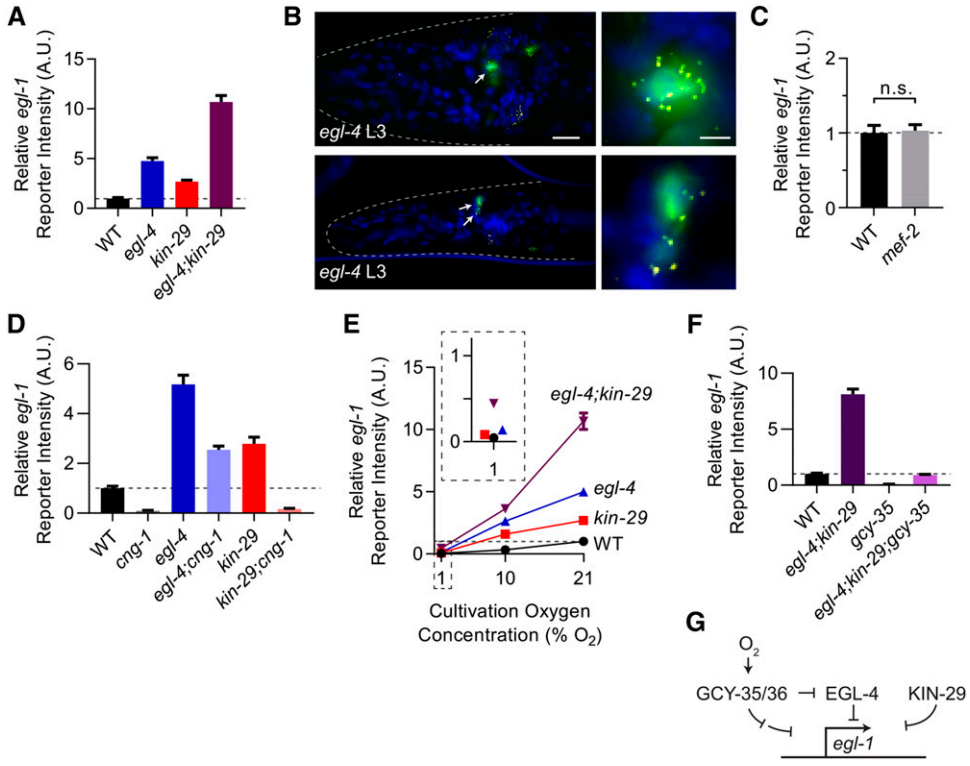

Figure 4 At least three pathways regulate *egl-1* expression in URX neurons. A. *egl-1* reporter expression at 21% oxygen in animals of the given genotype normalized to WT. Animals were synchronized by timed egg-laying and then imaged 3 days later. n ≥ 55 worms per genotype. Alleles used were *egl-4(n477)* and *kin-29(oy38)*. B. smFISH showing *egl-1* transcripts in *egl-4(n477)* mutant worms carrying the *muIs102* reporter (*Pgcy-32::GFP*) to label URX green. Blue is DAPI, *egl-1* mRNA transcripts are labeled yellow. Genotype and larval age of each animal is shown in white text. C. *egl-1* reporter expression in day 1 wild type and *mef-2(gv1)* worms at 21% oxygen, values normalized to wild type. n ≥ 45 worms per genotype. D. *egl-1* reporter expression in day 1 adult wild type, *cng-1(vx3)*, *egl-4(n477)*, *egl-4(n477);cng-1(jh111)*, *kin-29(oy38)*, and *cng-1(jh111);kin-29(oy38)* worms. *cng-1(vx3)* is a strong loss-of-function allele which fails to complement the *cng-1(jh111)* presumed null allele. E. *egl-1* reporter expression in the given genotypes at the given oxygen levels. Animals were synchronized by timed egg-laying and then imaged 3 days later. Values are normalized to wild-type worms grown at 21% oxygen. n ≥ 55 worms per genotype per condition. Alleles used were the same as in panel D. F. *egl-1* reporter expression in day 1 adult wild type, *egl-4(n477);kin-29(oy38)*, *gcy-35(ok769)*, and *egl-4(n477);kin-29(oy38);gcy-35(ok769)* mutant worms grown at 21% oxygen. Values are normalized to wild type, n ≥ 30 worms per genotype. G. Model showing a possible configuration of the relationship between oxygen sensation in URX and *egl-1* transcription. Arrows and lines do not imply direct interaction, only the valence and order of the genetic pathway. All error bars are 95% C.I. In photos, arrows indicate URX cell body and scale bars are 10 μm, except for the enlargements in panel B, in which the scale bar is 2 μm.

somatic cell deaths in the hermaphrodite worm cease, does not lead to cell death in any of the circumstances we examined.

In mammals, several BH3-only proteins are expressed in the adult animal in various tissues, including the nervous system (O'Reilly *et al.* 2000; Näpänkangas *et al.* 2003; Coultas *et al.* 2004; Sturm *et al.* 2006; Lein *et al.* 2007; Hawrylycz *et al.* 2012). It is difficult to assess the implication of this expression because many mammalian BH3-only proteins are regulated post-transcriptionally; however, this area of study is largely unexamined and could prove to be of significance. With at least eight family members, studying BH3-only proteins in mammals can be difficult due to redundancy in their functions (Giam *et al.* 2008). In contrast, *C. elegans* has only two BH3-only proteins, *egl-1* and *ced-13* (Schumacher *et al.* 2005). *egl-1* is necessary for nearly all developmental somatic cell deaths while CED-13 seems to function in germline cell death and does not appear to overlap with the activity of *egl-1* (Schumacher *et al.* 2005; King *et al.* 2018). These factors make studying the roles of BH3-only proteins more straightforward in *C. elegans*.

Intriguingly, transgenic expression of *egl-1* has been previously used to genetically ablate the URX neurons. The transgene array *qaIs2241* drives *egl-1* expression from the *gcy-36* promoter, and the death of URX in these animals was evident by both visual inspection and by URX-specific behavioral deficits (Chang *et al.* 2006; Styer *et al.* 2008; Carrillo *et al.* 2013; Zhao *et al.* 2018). Albeit artificial, this shows that URX is capable of undergoing apoptosis in an *egl-1*-dependent manner.

We propose that the most likely explanation for why this *egl-1* transgene array kills URX while the endogenous expression of *egl-1* we describe in this study does not is related to the expression level of *egl-1* in URX. The *gcy-36* gene is highly expressed in URX and *qaIs2241* contains multiple copies of *Pgcy-36::egl-1* in an array, so transgenic *egl-1* is likely expressed much higher than what occurs endogenously.

A recent study showed a threshold effect for *egl-1* expression, such that some cells during development transiently express very low levels of *egl-1* and do not die, but their daughter cells that do die highly upregulate *egl-1* to initiate cell death (Sherrard *et al.* 2017). This phenomenon could explain why URX survives development even though we can detect faint expression of our reporter in URX in eggs, when other cell deaths are occurring in the embryo.

egl-1 transcription in URX is regulated by neuronal activity, EGL-4, and/or KIN-29

We found that sensory transduction, the worm PKG homolog EGL-4, and the worm SIK homolog KIN-29 all regulate *egl-1* expression in URX in a complex manner. We did not directly test whether EGL-4 and KIN-29 act cell-autonomously in URX to regulate *egl-1*, which leaves open the possibility that they function in other cells to do so. Previous work has shown that both EGL-4 and KIN-29 can act in sensory neurons to cell-autonomously regulate chemoreceptor expression (Lanjuin and Sengupta 2002; Van Der Linden *et al.* 2008). Furthermore, the cellular localization of EGL-4 has previously been studied directly in AWC sensory neurons, where it was shown to translocate to the nucleus when intracellular cGMP decreased with prolonged exposure to an AWC-sensed odorant (O'Halloran *et al.* 2012). Interestingly, URX has a constitutively high level of cGMP in wild-type animals at 21% oxygen and even higher cGMP production in a *cng-1* mutant

background (Couto *et al.* 2013), yet our epistasis analysis found that EGL-4 repressed *egl-1* expression in URX when *cng-1* was mutated. This suggests that EGL-4 localization may be regulated differently in URX than in AWC, and that calcium entry may play a role. EGL-4 and KIN-29 have also been found to work together to regulate other activity-dependent genes, including several chemoreceptors in subsets of *C. elegans* neurons, such as the *str-1* chemoreceptor in the AWB sensory neuron (Van Der Linden *et al.* 2007; Van Der Linden *et al.* 2008). We found that, unlike how they are proposed to work in AWB to regulate expression of *str-1*, EGL-4 and KIN-29 likely do not act through the MEF-2 transcription factor to regulate *egl-1* expression. Also, the valence of expression for *egl-1* is opposite that of *str-1* in *egl-4* and *kin-29* mutants. That is, while *str-1* is downregulated in *egl-4* and *kin-29* mutants, *egl-1* is upregulated in these same genetic backgrounds. These differences with another known activity-dependent gene governed by *egl-4* and *kin-29* suggest that studying *egl-1* expression in URX can offer a complementary system to identify factors that regulate activity-dependent gene expression in *C. elegans*.

Both Protein Kinase G and the Salt-Inducible Kinase family have been shown to be involved in cell death regulation, in both repressive and activating roles in other model systems (Fiscus 2002; Deguchi *et al.* 2004; Cheng *et al.* 2009; Fallahian *et al.* 2011; Du *et al.* 2016; Tarumoto *et al.* 2018); however, their relation to BH3-only proteins has largely not been investigated. Our results suggest that exploring whether PKG and SIK family members regulate BH3-only proteins in other systems may be a worthwhile area of study. Though the transcription of *egl-1* in URX that we describe does not lead to apoptosis, it is feasible that these/such conserved regulators in other animals may have evolved a general or circumstantial role in programmed cell death.

The *egl-1* mutant is not impaired for multiple URX-related phenotypes

One important question that remains unanswered is whether or not the *egl-1* mRNA we see in URX is translated to a protein. We attempted to answer this question using a variety of approaches, such as immunohistochemistry using commercially available antibodies, tagging the endogenous protein with CRISPR, and transgenically expressing a tagged version of the protein. Unfortunately these attempts were unsuccessful, so we were unable to definitively assess whether the *egl-1* protein product is present in URX. Other labs have also reported being unable to tag the *egl-1* protein (B. Conradt, personal communication).

Despite the lack of a clear answer about the presence of *egl-1* protein in URX, we nevertheless compared the *egl-1* mutant and wild-type worms with regard to the known URX-related functions of oxygen sensation and immune response to pathogenic bacteria. For both cases, we found no differences. We also examined URX at the cellular level in the *egl-1* mutant by looking at dendrite and synapse morphology. General synapse morphology looked normal in the *egl-1* mutant, though there was a slight defect in dendritic tip morphology compared to wild type. However, this defect could have several origins that are unrelated to an action of *egl-1* in URX, so we did not follow this subtle phenotype further.

In the absence of a clear abnormal phenotype of the *egl-1* mutant with regard to URX function, we can only speculate about why *egl-1* is transcribed in this living pair of neurons. One possibility is that whereas *egl-1* normally triggers cell death during development, its expression in URX represents an atypically regulated form of apoptosis for which the *egl-1* transcript is maintained in the cell so that in response to some additional trigger the translated protein product then induces apoptosis. There is at least one other example for which *egl-1* expression does not cause immediate cell death (Johnsen and Horvitz 2016); the cell B.al/rapaav in the male tail expresses *egl-1* but persists in a poised state unless a neighboring cell begins to engulf it, at which point cell death occurs – a process termed "assisted suicide." The URX neuron pair might similarly exist in a poised state in the wild-type worm. In this model, one or more unknown signals would act as the "trigger" that causes translation of *egl-1* and possibly cell death. Because wild isolates of *C. elegans* typically prefer 5–12% O_2 conditions and URX is tonically active, one trigger might be prolonged exposure to higher concentrations of oxygen. However, URX neurons show no evidence of death or dysfunction when cultivated at 21% or 100% oxygen. Also, we found that exposure to 100% oxygen did not lead to higher *egl-1* reporter expression than at 21% oxygen. Thus, high oxygen levels do not appear to serve as an apoptotic trigger for URX, at least alone.

One potential problem with this apoptotic-trigger hypothesis, however, is that the canonical downstream binding partner of *egl-1*, CED-9, and the downstream effector CED-4 are both thought to no longer be expressed in somatic tissue past early development (Chen *et al.* 2000), so *egl-1* protein expressed in URX in late larval and adult *C. elegans* might not induce apoptosis.

An alternate possibility is that *egl-1* expression in URX represents a moonlighting function for *egl-1*, similar to the non-apoptotic roles that are beginning to be uncovered for mammalian BH3-only proteins (Esposti *et al.* 2001; Danial *et al.* 2003; Maiuri *et al.* 2007; Danial *et al.* 2008; Sinha *et al.* 2008; Giménez-Cassina *et al.* 2014; Lindqvist *et al.* 2014). The apoptotic-trigger and moonlighting possibilities are not mutually exclusive.

Activity-dependent *egl-1* transcription in post-developmental *C. elegans* might provide a new system for the study of mechanisms that regulate activity-dependent gene expression and might also possibly reveal a non-apoptotic role for a BH3-only protein. Our future work will focus on identifying the mechanisms and transcription factors by which neuronal activity controls *egl-1* transcription in URX, and on what role *egl-1* might play in this neuron.

ACKNOWLEDGMENTS

We would like to thank Lina Gomez and Luisa Scott for helpful discussions, Michael Nonet for reagents, and Susan Rozmiarek for expert assistance. Some strains were provided by the CGC, which is funded by NIH Office of Research Infrastructure Programs (P40 OD010440). Additional funds were provided by NIH-NIA grants RF1AG057355 and R01AG041135. V.K.D. was a Howard Hughes Medical Institute International Student Research fellow. H.R.H. is an Investigator of the Howard Hughes Medical Institute.

LITERATURE CITED

Aouacheria, A., F. Brunet, and M. Gouy, 2005 Phylogenomics of life-or-death switches in multicellular animals: Bcl-2, BH3-Only, and BNip families of apoptotic regulators. Mol. Biol. Evol. 22: 2395–2416. https://doi.org/10.1093/molbev/msi234

Borensztajn, K. S., M. F. Bijlsma, A. P. Groot, L. W. Bruggemann, H. H. Versteeg *et al.*, 2007 Coagulation factor Xa drives tumor cells into apoptosis through BH3-only protein Bim up-regulation. Exp. Cell Res. 313: 2622–2633. https://doi.org/10.1016/j.yexcr.2007.04.014

Boulin, T., J. F. Etchberger, and O. Hobert, 2006 Reporter gene fusions. WormBook 1–23. http://doi/10.1895/wormbook.1.106.1, http://www.wormbook.org.

Bounoutas, A., Q. Zheng, M. L. Nonet and M. Chalfie, 2009 *mec-15* encodes an F-box protein required for touch receptor neuron mechanosensation, synapse formation and development. Genetics 183: 607–617, 601SI-604SI.

Busch, K. E., P. Laurent, Z. Soltesz, R. J. Murphy, O. Faivre *et al.*, 2012 Tonic signaling from O(2) sensors sets neural circuit activity and behavioral state. Nat. Neurosci. 15: 581–591. https://doi.org/10.1038/nn.3061

Carrillo, M. A., M. L. Guillermin, S. Rengarajan, R. P. Okubo, and E. A. Hallem, 2013 O2-sensing neurons control CO2 response in *C. elegans*. J. Neurosci. 33: 9675–9683. https://doi.org/10.1523/JNEUROSCI.4541-12.2013

Chang, A. J., N. Chronis, D. S. Karow, M. A. Marletta, and C. I. Bargmann, 2006 A distributed chemosensory circuit for oxygen preference in *C. elegans*. PLoS Biol. 4: e274. https://doi.org/10.1371/journal.pbio.0040274

Chen, F., B. M. Hersh, B. Conradt, Z. Zhou, D. Riemer *et al.*, 2000 Translocation of *C. elegans* CED-4 to nuclear membranes during programmed cell death. Science 287: 1485–1489. https://doi.org/10.1126/science.287.5457.1485

Cheng, H., P. Liu, Z. C. Wang, L. Zou, S. Santiago *et al.*, 2009 SIK1 couples LKB1 to p53-dependent anoikis and suppresses metastasis. Sci. Signal. 2: ra35. https://doi.org/10.1126/scisignal.2000369

Cheung, B. H., F. Arellano-Carbajal, I. Rybicki, and M. de Bono, 2004 Soluble guanylate cyclases act in neurons exposed to the body fluid to promote *C. elegans* aggregation behavior. Curr. Biol. 14: 1105–1111. https://doi.org/10.1016/j.cub.2004.06.027

Cho, S. W., J. H. Cho, H. O. Song, and C. S. Park, 2005 Identification and characterization of a putative cyclic nucleotide-gated channel, CNG-1, in *C. elegans*. Mol. Cells 19: 149–154.

Conradt, B., and H. R. Horvitz, 1998 The *C. elegans* protein EGL-1 is required for programmed cell death and interacts with the Bcl-2-like protein CED-9. Cell 93: 519–529. https://doi.org/10.1016/S0092-8674(00)81182-4

Conradt, B., and H. R. Horvitz, 1999 The TRA-1A sex determination protein of *C. elegans* regulates sexually dimorphic cell deaths by repressing the egl-1 cell death activator gene. Cell 98: 317–327. https://doi.org/10.1016/S0092-8674(00)81961-3

Coultas, L., P. Bouillet, E. G. Stanley, T. C. Brodnicki, J. M. Adams *et al.*, 2004 Proapoptotic BH3-only Bcl-2 family member Bik/Blk/Nbk is expressed in hemopoietic and endothelial cells but is redundant for their programmed death. Mol. Cell. Biol. 24: 1570–1581. https://doi.org/10.1128/MCB.24.4.1570-1581.2004

Couto, A., S. Oda, V. O. Nikolaev, Z. Soltesz, and M. de Bono, 2013 In vivo genetic dissection of O2-evoked cGMP dynamics in a *Caenorhabditis elegans* gas sensor. Proc. Natl. Acad. Sci. USA 110: E3301–E3310. https://doi.org/10.1073/pnas.1217428110

Czabotar, P. E., G. Lessene, A. Strasser, and J. M. Adams, 2014 Control of apoptosis by the BCL-2 protein family: implications for physiology and therapy. Nat. Rev. Mol. Cell Biol. 15: 49–63. https://doi.org/10.1038/nrm3722

Danial, N. N., C. F. Gramm, L. Scorrano, C. Y. Zhang, S. Krauss *et al.*, 2003 BAD and glucokinase reside in a mitochondrial complex that integrates glycolysis and apoptosis. Nature 424: 952–956. https://doi.org/10.1038/nature01825

Danial, N. N., L. D. Walensky, C. Y. Zhang, C. S. Choi, J. K. Fisher *et al.*, 2008 Dual role of proapoptotic BAD in insulin secretion and beta cell survival. Nat. Med. 14: 144–153. https://doi.org/10.1038/nm1717

Daniels, S. A., M. Ailion, J. H. Thomas, and P. Sengupta, 2000 *egl-4* acts through a transforming growth factor-beta/SMAD pathway in *Caenorhabditis* elegans to regulate multiple neuronal circuits in response to sensory cues. Genetics 156: 123–141.

de Bono, M., and C. I. Bargmann, 1998 Natural variation in a neuropeptide Y receptor homolog modifies social behavior and food response in *C. elegans*. Cell 94: 679–689. https://doi.org/10.1016/S0092-8674(00)81609-8

Deguchi, A., W. J. Thompson, and I. B. Weinstein, 2004 Activation of protein kinase G is sufficient to induce apoptosis and inhibit cell migration in colon cancer cells. Cancer Res. 64: 3966–3973. https://doi.org/10.1158/0008-5472.CAN-03-3740

Deniaud, E., J. Baguet, A. L. Mathieu, G. Pages, J. Marvel *et al.*, 2006 Overexpression of Sp1 transcription factor induces apoptosis. Oncogene 25: 7096–7105. https://doi.org/10.1038/sj.onc.1209696

Doroquez, D. B., C. Berciu, J. R. Anderson, P. Sengupta, and D. Nicastro, 2014 A high-resolution morphological and ultrastructural map of anterior sensory cilia and glia in *Caenorhabditis elegans*. eLife 3: e01948. https://doi.org/10.7554/eLife.01948

Du, W. Q., J. N. Zheng, and D. S. Pei, 2016 The diverse oncogenic and tumor suppressor roles of salt-inducible kinase (SIK) in cancer. Expert Opin. Ther. Targets 20: 477–485. https://doi.org/10.1517/14728222.2016.1101452

Ellis, H. M., and H. R. Horvitz, 1986 Genetic control of programmed cell death in the nematode *C. elegans*. Cell 44: 817–829. https://doi.org/10.1016/0092-8674(86)90004-8

Ellis, R. E., and H. R. Horvitz, 1991 Two *C. elegans* genes control the programmed deaths of specific cells in the pharynx. Development 112: 591–603.

Esposti, M. D., J. T. Erler, J. A. Hickman, and C. Dive, 2001 Bid, a widely expressed proapoptotic protein of the *Bcl-2* family, displays lipid transfer activity. Mol. Cell. Biol. 21: 7268–7276. https://doi.org/10.1128/MCB.21.21.7268-7276.2001

Fallahian, F., F. Karami-Tehrani, S. Salami, and M. Aghaei, 2011 Cyclic GMP induced apoptosis via protein kinase G in oestrogen receptor-positive and -negative breast cancer cell lines. FEBS J. 278: 3360–3369. https://doi.org/10.1111/j.1742-4658.2011.08260.x

Fiscus, R. R., 2002 Involvement of cyclic GMP and protein kinase G in the regulation of apoptosis and survival in neural cells. Neurosignals 11: 175–190. https://doi.org/10.1159/000065431

Giam, M., D. C. Huang, and P. Bouillet, 2008 BH3-only proteins and their roles in programmed cell death. Oncogene 27: S128–S136. https://doi.org/10.1038/onc.2009.50

Giménez-Cassina, A., L. Garcia-Haro, C. S. Choi, M. A. Osundiji, E. A. Lane *et al.*, 2014 Regulation of hepatic energy metabolism and gluconeogenesis by BAD. Cell Metab. 19: 272–284. https://doi.org/10.1016/j.cmet.2013.12.001

Ginsberg, D., 2002 E2F1 pathways to apoptosis. FEBS Lett. 529: 122–125. https://doi.org/10.1016/S0014-5793(02)03270-2

Gray, J. M., D. S. Karow, H. Lu, A. J. Chang, J. S. Chang *et al.*, 2004 Oxygen sensation and social feeding mediated by a *C. elegans* guanylate cyclase homologue. Nature 430: 317–322. https://doi.org/10.1038/nature02714

Happo, L., A. Strasser, and S. Cory, 2012 BH3-only proteins in apoptosis at a glance. J. Cell Sci. 125: 1081–1087. https://doi.org/10.1242/jcs.090514

Hawrylycz, M. J., E. S. Lein, A. L. Guillozet-Bongaarts, E. H. Shen, L. Ng *et al.*, 2012 An anatomically comprehensive atlas of the adult human brain transcriptome. Nature 489: 391–399. https://doi.org/10.1038/nature11405

Hengartner, M. O., R. E. Ellis, and H. R. Horvitz, 1992 *Caenorhabditis elegans* gene ced-9 protects cells from programmed cell death. Nature 356: 494–499. https://doi.org/10.1038/356494a0

Hirose, T., B. D. Galvin, and H. R. Horvitz, 2010 Six and Eya promote apoptosis through direct transcriptional activation of the proapoptotic BH3-only gene *egl-1* in *Caenorhabditis elegans*. Proc. Natl. Acad. Sci. USA 107: 15479–15484. https://doi.org/10.1073/pnas.1010023107

Hirose, T., and H. R. Horvitz, 2013 An *Sp1* transcription factor coordinates caspase-dependent and -independent apoptotic pathways. Nature 500: 354–358. https://doi.org/10.1038/nature12329

Jang, H., S. Levy, S. W. Flavell, F. Mende, R. Latham *et al.*, 2017 Dissection of neuronal gap junction circuits that regulate social behavior in *Caenorhabditis elegans*. Proc. Natl. Acad. Sci. USA 114: E1263–E1272. https://doi.org/10.1073/pnas.1621274114

Johnsen, H. L., and H. R. Horvitz, 2016 Both the apoptotic suicide pathway and phagocytosis are required for a programmed cell death in *Caenorhabditis elegans*. BMC Biol. 14: 39. https://doi.org/10.1186/s12915-016-0262-5

Katoh, Y., H. Takemori, J. Doi, and M. Okamoto, 2002 Identification of the nuclear localization domain of salt-inducible kinase. Endocr. Res. 28: 315–318. https://doi.org/10.1081/ERC-120016802

King, S. D., C. F. Gray, L. Song, R. Nechushtai, T. L. Gumienny *et al.*, 2019 The cisd gene family regulates physiological germline apoptosis through *ced-13* and the canonical cell death pathway in *Caenorhabditis elegans*. Cell Death Differ. 26: 162–178. https://doi.org/10.1038/s41418-018-0108-5

L'Etoile, N. D., C. M. Coburn, J. Eastham, A. Kistler, G. Gallegos *et al.*, 2002 The cyclic GMP-dependent protein kinase EGL-4 regulates olfactory adaptation in *C. elegans*. Neuron 36: 1079–1089. https://doi.org/10.1016/S0896-6273(02)01066-8

Lainé, V., J. R. Ségor, H. Zhan, J. L. Bessereau, and M. Jospin, 2014 Hyperactivation of L-type voltage-gated Ca2+ channels in *Caenorhabditis elegans* striated muscle can result from point mutations in the IS6 or the IIIS4 segment of the α1 subunit. J. Exp. Biol. 217: 3805–3814. https://doi.org/10.1242/jeb.106732

Lanjuin, A., and P. Sengupta, 2002 Regulation of chemosensory receptor expression and sensory signaling by the KIN-29 Ser/Thr kinase. Neuron 33: 369–381. https://doi.org/10.1016/S0896-6273(02)00572-X

Lein, E. S., M. J. Hawrylycz, N. Ao, M. Ayres, A. Bensinger *et al.*, 2007 Genome-wide atlas of gene expression in the adult mouse brain. Nature 445: 168–176. https://doi.org/10.1038/nature05453

Lettre, G., and M. O. Hengartner, 2006 Developmental apoptosis in *C. elegans*: a complex CEDnario. Nat. Rev. Mol. Cell Biol. 7: 97–108. https://doi.org/10.1038/nrm1836

Lindqvist, L. M., M. Heinlein, D. C. Huang, and D. L. Vaux, 2014 Prosurvival Bcl-2 family members affect autophagy only indirectly, by inhibiting Bax and Bak. Proc. Natl. Acad. Sci. USA 111: 8512–8517. https://doi.org/10.1073/pnas.1406425111

Liu, H., T. J. Strauss, M. B. Potts, and S. Cameron, 2006 Direct regulation of egl-1 and of programmed cell death by the Hox protein MAB-5 and by CEH-20, a *C. elegans* homolog of Pbx1. Development 133: 641–650. https://doi.org/10.1242/dev.02234

Liu, Q. A., and M. O. Hengartner, 1998 Candidate adaptor protein CED-6 promotes the engulfment of apoptotic cells in *C. elegans*. Cell 93: 961–972. https://doi.org/10.1016/S0092-8674(00)81202-7

Lomonosova, E., and G. Chinnadurai, 2008 BH3-only proteins in apoptosis and beyond: an overview. Oncogene 27: S2–S19. https://doi.org/10.1038/onc.2009.39

Lowman, X. H., M. A. McDonnell, A. Kosloske, O. A. Odumade, C. Jenness *et al.*, 2010 The proapoptotic function of Noxa in human leukemia cells is regulated by the kinase Cdk5 and by glucose. Mol. Cell 40: 823–833. https://doi.org/10.1016/j.molcel.2010.11.035

Maiuri, M. C., A. Criollo, E. Tasdemir, J. M. Vicencio, N. Tajeddine *et al.*, 2007 BH3-only proteins and BH3 mimetics induce autophagy by competitively disrupting the interaction between Beclin 1 and Bcl-2/Bcl-X(L). Autophagy 3: 374–376. https://doi.org/10.4161/auto.4237

Mariol, M. C., L. Walter, S. Bellemin, and K. Gieseler, 2013 A rapid protocol for integrating extrachromosomal arrays with high transmission rate into the *C. elegans* genome. J. Vis. Exp. 82: e50773. https://doi.org/10.3791/50773

McCloy, R. A., S. Rogers, C. E. Caldon, T. Lorca, A. Castro *et al.*, 2014 Partial inhibition of Cdk1 in G 2 phase overrides the SAC and decouples mitotic events. Cell Cycle 13: 1400–1412. https://doi.org/10.4161/cc.28401

Meng, L., B. Mulcahy, S. J. Cook, M. Neubauer, A. Wan *et al.*, 2015 The Cell Death Pathway Regulates Synapse Elimination through Cleavage of Gelsolin in *Caenorhabditis elegans* Neurons. Cell Reports 11: 1737–1748. https://doi.org/10.1016/j.celrep.2015.05.031

Metzstein, M. M., M. O. Hengartner, N. Tsung, R. E. Ellis, and H. R. Horvitz, 1996 Transcriptional regulator of programmed cell death encoded by *Caenorhabditis elegans* gene ces-2. Nature 382: 545–547. https://doi.org/10.1038/382545a0

Nagai, T., S. Yamada, T. Tominaga, M. Ichikawa, and A. Miyawaki, 2004 Expanded dynamic range of fluorescent indicators for Ca(2+) by circularly permuted yellow fluorescent proteins. Proc. Natl. Acad. Sci. USA 101: 10554–10559. https://doi.org/10.1073/pnas.0400417101

Nakano, K., and K. H. Vousden, 2001 PUMA, a novel proapoptotic gene, is induced by p53. Mol. Cell 7: 683–694. https://doi.org/10.1016/S1097-2765(01)00214-3

Näpänkangas, U., N. Lindqvist, D. Lindholm, and F. Hallbook, 2003 Rat retinal ganglion cells upregulate the pro-apoptotic BH3-only protein Bim after optic nerve transection. Brain Res. Mol. Brain Res. 120: 30–37. https://doi.org/10.1016/j.molbrainres.2003.09.016

Nehme, R., and B. Conradt, 2008 egl-1: a key activator of apoptotic cell death in *C. elegans*. Oncogene 27: S30–S40. https://doi.org/10.1038/onc.2009.41

Nehme, R., P. Grote, T. Tomasi, S. Loser, H. Holzkamp *et al.*, 2010 Transcriptional upregulation of both egl-1 BH3-only and ced-3 caspase is required for the death of the male-specific CEM neurons. Cell Death Differ. 17: 1266–1276. https://doi.org/10.1038/cdd.2010.3

O'Halloran, D. M., O. S. Hamilton, J. I. Lee, M. Gallegos, and N. D. L'Etoile, 2012 Changes in cGMP levels affect the localization of EGL-4 in AWC in *Caenorhabditis elegans*. PLoS One 7: e31614. https://doi.org/10.1371/journal.pone.0031614

O'Reilly, L. A., L. Cullen, J. Visvader, G. J. Lindeman, C. Print *et al.*, 2000 The proapoptotic BH3-only protein bim is expressed in hematopoietic, epithelial, neuronal, and germ cells. Am. J. Pathol. 157: 449–461. https://doi.org/10.1016/S0002-9440(10)64557-9

Oda, E., R. Ohki, H. Murasawa, J. Nemoto, T. Shibue *et al.*, 2000 Noxa, a BH3-only member of the Bcl-2 family and candidate mediator of p53-induced apoptosis. Science 288: 1053–1058. https://doi.org/10.1126/science.288.5468.1053

Parker, P. J., and S. J. Parkinson, 2001 AGC protein kinase phosphorylation and protein kinase C. Biochem. Soc. Trans. 29: 860–863. https://doi.org/10.1042/bst0290860

Potts, M. B., D. P. Wang, and S. Cameron, 2009 Trithorax, Hox, and TALE-class homeodomain proteins ensure cell survival through repression of the BH3-only gene egl-1. Dev. Biol. 329: 374–385. https://doi.org/10.1016/j.ydbio.2009.02.022

Raj, A., P. van den Bogaard, S. A. Rifkin, A. van Oudenaarden, and S. Tyagi, 2008 Imaging individual mRNA molecules using multiple singly labeled probes. Nat. Methods 5: 877–879. https://doi.org/10.1038/nmeth.1253

Ruiz i Altaba, A., P. Sanchez, and N. Dahmane, 2002 Gli and hedgehog in cancer: tumours, embryos and stem cells. Nat. Rev. Cancer 2: 361–372. https://doi.org/10.1038/nrc796

Schumacher, B., C. Schertel, N. Wittenburg, S. Tuck, S. Mitani *et al.*, 2005 *C. elegans ced-13* can promote apoptosis and is induced in response to DNA damage. Cell Death Differ. 12: 153–161 (erratum: Cell Death Differ. 12: 532). https://doi.org/10.1038/sj.cdd.4401539

Shaham, S., and H. R. Horvitz, 1996 Developing *Caenorhabditis elegans* neurons may contain both cell-death protective and killer activities. Genes Dev. 10: 578–591. https://doi.org/10.1101/gad.10.5.578

Sherrard, R., S. Luehr, H. Holzkamp, K. McJunkin, N. Memar *et al.*, 2017 miRNAs cooperate in apoptosis regulation during *C. elegans* development. Genes Dev. 31: 209–222. https://doi.org/10.1101/gad.288555.116

Shevchuk, N. A., A. V. Bryksin, Y. A. Nusinovich, F. C. Cabello, M. Sutherland *et al.*, 2004 Construction of long DNA molecules using long PCR-based fusion of several fragments simultaneously. Nucleic Acids Res. 32: e19. https://doi.org/10.1093/nar/gnh014

Sinha, S., C. L. Colbert, N. Becker, Y. Wei, and B. Levine, 2008 Molecular basis of the regulation of Beclin 1-dependent autophagy by the gamma-herpesvirus 68 Bcl-2 homolog M11. Autophagy 4: 989–997 (erratum: Autophagy 5: 284). https://doi.org/10.4161/auto.6803

Sitwala, K. V., M. N. Dandekar, and J. L. Hess, 2008 HOX proteins and leukemia. Int. J. Clin. Exp. Pathol. 1: 461–474.

Stansberry, J., E. J. Baude, M. K. Taylor, P. J. Chen, S. W. Jin *et al.*, 2001 A cGMP-dependent protein kinase is implicated in wild-type motility in *C. elegans*. J. Neurochem. 76: 1177–1187. https://doi.org/10.1046/j.1471-4159.2001.00131.x

Sturm, I., C. Stephan, B. Gillissen, R. Siebert, M. Janz *et al.*, 2006 Loss of the tissue-specific proapoptotic BH3-only protein Nbk/Bik is a unifying feature of renal cell carcinoma. Cell Death Differ. 13: 619–627. https://doi.org/10.1038/sj.cdd.4401782

Styer, K. L., V. Singh, E. Macosko, S. E. Steele, C. I. Bargmann *et al.*, 2008 Innate immunity in *Caenorhabditis elegans* is regulated by neurons expressing NPR-1/GPCR. Science 322: 460–464. https://doi.org/10.1126/science.1163673

Sulston, J. E., and H. R. Horvitz, 1977 Post-embryonic cell lineages of the nematode, *Caenorhabditis elegans*. Dev. Biol. 56: 110–156. https://doi.org/10.1016/0012-1606(77)90158-0

Tarumoto, Y., B. Lu, T. D. D. Somerville, Y. H. Huang, J. P. Milazzo *et al.*, 2018 LKB1, Salt-Inducible Kinases, and MEF2C Are Linked Dependencies in Acute Myeloid Leukemia. Mol Cell 69**:** 1017–1027 e1016.

Taylor, S. R., G. Santpere, M. Reilly, L. Glenwinkel, A. Poff *et al.*, 2019 Expression profiling of the mature *C. elegans* nervous system by

single-cell RNA-Sequencing. bioRxiv. https://www.biorxiv.org/content/10.1101/737577v2

Thellmann, M., J. Hatzold, and B. Conradt, 2003 The Snail-like CES-1 protein of *C. elegans* can block the expression of the BH3-only cell-death activator gene egl-1 by antagonizing the function of bHLH proteins. Development 130: 4057–4071. https://doi.org/10.1242/dev.00597

Tursun, B., L. Cochella, I. Carrera, and O. Hobert, 2009 A toolkit and robust pipeline for the generation of fosmid-based reporter genes in *C. elegans*. PLoS One 4: e4625. https://doi.org/10.1371/journal.pone.0004625

van der Linden, A. M., K. M. Nolan, and P. Sengupta, 2007 KIN-29 SIK regulates chemoreceptor gene expression via an MEF2 transcription factor and a class II HDAC. EMBO J. 26: 358–370. https://doi.org/10.1038/sj.emboj.7601479

van der Linden, A. M., S. Wiener, Y. J. You, K. Kim, L. Avery *et al.*, 2008 The EGL-4 PKG acts with KIN-29 salt-inducible kinase and protein kinase A to regulate chemoreceptor gene expression and sensory behaviors in *Caenorhabditis elegans*. Genetics 180: 1475–1491. https://doi.org/10.1534/genetics.108.094771

Ventura, A., A. G. Young, M. M. Winslow, L. Lintault, A. Meissner *et al.*, 2008 Targeted deletion reveals essential and overlapping functions of the miR-17 through 92 family of miRNA clusters. Cell 132: 875–886. https://doi.org/10.1016/j.cell.2008.02.019

Verma, S., L. J. Zhao, and G. Chinnadurai, 2001 Phosphorylation of the pro-apoptotic protein BIK: mapping of phosphorylation sites and effect on apoptosis. J. Biol. Chem. 276: 4671–4676. https://doi.org/10.1074/jbc.M008983200

Wallis, D. E., E. Roessler, U. Hehr, L. Nanni, T. Wiltshire *et al.*, 1999 Mutations in the homeodomain of the human SIX3 gene cause holoprosencephaly. Nat. Genet. 22: 196–198. https://doi.org/10.1038/9718

Ward, S., N. Thomson, J. G. White, and S. Brenner, 1975 Electron microscopical reconstruction of the anterior sensory anatomy of the nematode *Caenorhabditis elegans*.?2UU. J. Comp. Neurol. 160: 313–337. https://doi.org/10.1002/cne.901600305

White, J. G., E. Southgate, J. N. Thomson, and S. Brenner, 1986 The structure of the nervous system of the nematode *Caenorhabditis elegans*. Philos. Trans. R. Soc. Lond. B Biol. Sci. 314: 1–340. https://doi.org/10.1098/rstb.1986.0056

Winn, J., M. Carter, L. Avery, and S. Cameron, 2011 Hox and a newly identified E2F co-repress cell death in *Caenorhabditis elegans*. Genetics 188: 897–905. https://doi.org/10.1534/genetics.111.128421

Witham, E., C. Comunian, H. Ratanpal, S. Skora, M. Zimmer *et al.*, 2016 *C. elegans* Body Cavity Neurons Are Homeostatic Sensors that Integrate Fluctuations in Oxygen Availability and Internal Nutrient Reserves. Cell Reports 14: 1641–1654. https://doi.org/10.1016/j.celrep.2016.01.052

Wojtyniak, M., A. G. Brear, D. M. O'Halloran, and P. Sengupta, 2013 Cell- and subunit-specific mechanisms of CNG channel ciliary trafficking and localization in *C. elegans*. J. Cell Sci. 126: 4381–4395. https://doi.org/10.1242/jcs.127274

Wong, P., M. Iwasaki, T. C. Somervaille, C. W. So, and M. L. Cleary, 2007 Meis1 is an essential and rate-limiting regulator of MLL leukemia stem cell potential. Genes Dev. 21: 2762–2774. https://doi.org/10.1101/gad.1602107

Wu, W. S., S. Heinrichs, D. Xu, S. P. Garrison, G. P. Zambetti *et al.*, 2005 Slug antagonizes p53-mediated apoptosis of hematopoietic progenitors by repressing puma. Cell 123: 641–653. https://doi.org/10.1016/j.cell.2005.09.029

Xu, P. X., J. Adams, H. Peters, M. C. Brown, S. Heaney *et al.*, 1999 Eya1-deficient mice lack ears and kidneys and show abnormal apoptosis of organ primordia. Nat. Genet. 23: 113–117. https://doi.org/10.1038/12722

Yu, S., L. Avery, E. Baude, and D. L. Garbers, 1997 Guanylyl cyclase expression in specific sensory neurons: a new family of chemosensory receptors. Proc. Natl. Acad. Sci. USA 94: 3384–3387. https://doi.org/10.1073/pnas.94.7.3384

Yuan, J., and H. R. Horvitz, 1992 The *Caenorhabditis elegans* cell death gene ced-4 encodes a novel protein and is expressed during the period of extensive programmed cell death. Development 116: 309–320.

Yuan, J. Y., and H. R. Horvitz, 1990 The *Caenorhabditis elegans* genes ced-3 and ced-4 act cell autonomously to cause programmed cell death. Dev. Biol. 138: 33–41. https://doi.org/10.1016/0012-1606(90)90174-H

Zhao, Y., L. Long, W. Xu, R. F. Campbell, E. E. Large *et al.*, 2018 Changes to social feeding behaviors are not sufficient for fitness gains of the *Caenorhabditis elegans* N2 reference strain. eLife 7. https://doi.org/10.7554/eLife.38675

Zimmer, M., J. M. Gray, N. Pokala, A. J. Chang, D. S. Karow *et al.*, 2009 Neurons detect increases and decreases in oxygen levels using distinct guanylate cyclases. Neuron 61: 865–879. https://doi.org/10.1016/j.neuron.2009.02.013

Zuryn, S., S. Le Gras, K. Jamet, and S. Jarriault, 2010 A strategy for direct mapping and identification of mutations by whole-genome sequencing. Genetics 186: 427–430. https://doi.org/10.1534/genetics.110.119230

Communicating editor: S. Lee